

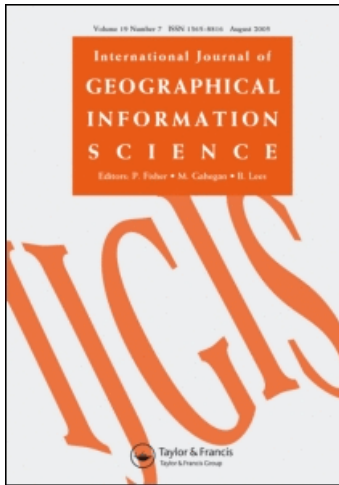
This article was downloaded by: [University of Colorado, Boulder campus]

On: 15 July 2009

Access details: Access Details: [subscription number 785022308]

Publisher Taylor & Francis

Informa Ltd Registered in England and Wales Registered Number: 1072954 Registered office: Mortimer House, 37-41 Mortimer Street, London W1T 3JH, UK



International Journal of Geographical Information Science

Publication details, including instructions for authors and subscription information:

<http://www.informaworld.com/smpp/title~content=t71359799>

Multi-scale and multi-criteria mapping of mountain peaks as fuzzy entities

Y. Deng ^a; J. P. Wilson ^b

^a Department of Geography, Western Illinois University, Macomb, USA ^b Department of Geography, University of Southern California, Los Angeles, USA

First Published on: 16 July 2007

To cite this Article Deng, Y. and Wilson, J. P. (2007) 'Multi-scale and multi-criteria mapping of mountain peaks as fuzzy entities', *International Journal of Geographical Information Science*, 22:2, 205 — 218

To link to this Article: DOI: 10.1080/13658810701405623

URL: <http://dx.doi.org/10.1080/13658810701405623>

PLEASE SCROLL DOWN FOR ARTICLE

Full terms and conditions of use: <http://www.informaworld.com/terms-and-conditions-of-access.pdf>

This article may be used for research, teaching and private study purposes. Any substantial or systematic reproduction, re-distribution, re-selling, loan or sub-licensing, systematic supply or distribution in any form to anyone is expressly forbidden.

The publisher does not give any warranty express or implied or make any representation that the contents will be complete or accurate or up to date. The accuracy of any instructions, formulae and drug doses should be independently verified with primary sources. The publisher shall not be liable for any loss, actions, claims, proceedings, demand or costs or damages whatsoever or howsoever caused arising directly or indirectly in connection with or arising out of the use of this material.

Research Article

Multi-scale and multi-criteria mapping of mountain peaks as fuzzy entities

Y. DENG*† and J. P. WILSON‡

†Department of Geography, Western Illinois University, Macomb, IL 61455-1390, USA

‡Department of Geography, University of Southern California, Los Angeles, CA 90089-0255, USA

(Received 2 July 2006; in final form 27 March 2007)

Mountain peaks are mapped as multi-scale entities with modifiable boundaries and variable contents. Four semantic meanings are imported and quantified to first characterize peaks at a range of spatial scales and then evaluate the multi-criteria 'peakness' at each scale. Peakness is defined as the prototypicality of identified summits and as the similarity of each point (cell) to summits. The procedure then summarizes the individual-scale peakness across considered spatial scales into a univariate membership surface. This allows mapping of vague peak entities as non-homogeneous peak regions whose boundaries depend on user-specified peakness thresholds. This procedure was applied in a case study to tackle several challenges in landform delineation, including boundary, spatial continuity, spatial scale, topographic context, and multi-criteria definition.

Keywords: Peaks; Multi-scale; Fuzzy; Criteria; Santa Monica Mountains

1. Introduction

Terrain surfaces usually exist as spatial continua and 'individual landforms are seldom bona fide objects with crisp boundaries of their own' (Smith and Mark 2003; also see Wood 1998, Fisher *et al.* 2005). For instance, mountain peaks demonstrate spatial gradation to surrounding hillslopes, thematic similarity to ridges, and fuzzy distinctions with hills or mountains that contain peaks (Mark and Smith 2004, Schmidt and Hewitt 2004). A locally prominent peak may (or may not) become unimportant when observed at a much farther distance. The diverse real-world meanings of peaks (e.g. for pilots, scientists, mountain climbers, and wildfire fighters) imply additional variations in thematic criteria and geographic delineation. Vagueness thus exists not only for peak boundaries, but also for the central concept 'peak' itself (Fisher *et al.*, in press). A realistic GIS representation of peaks should therefore simultaneously take into account: (1) the spatial continuity of terrain surfaces; (2) the multi-criteria and non-uniform peak perceptions; and (3) the multi-scale and contextual (nesting and nested) nature of topography. This paper focuses on these goals and describes a procedure that maps peaks as multi-scale, multi-criteria fuzzy spatial entities.

*Corresponding author. Email: y-deng2@wiu.edu

2. Related literature

Mackay *et al.* (1992) advocated use of higher-order geographic objects (HOGO), rather than just cells, for topographic characterization, and they incorporated inexact reasoning to indicate the fuzzy certainty level of the resultant delineations. Graff and Usery (1993) distinguished prototype 'mounts' from non-prototype mounts after translating the qualitative definition of mount into a series of quantitative rules. Usery (1996) later used elevation to derive mount memberships. These efforts represent early implementations of SI (semantic import) fuzzy sets (Burrough and McDonnell 1998, pp. 270–273), and they typically characterize landforms in a simplified way and at a narrow range of spatial scales. Wood (2004) suggests using *relative drop* (*rd*) to quantitatively compare peak memberships and to represent nested, multi-scale peaks. *rd* addresses the multi-scale topographic position well, but it is difficult to use this single criterion to represent rich surface morphometric characteristics.

Fisher *et al.* (2004, 2005) assigned each grid point to a morphometric class—pit, peak, pass, ridge, channel, or plane—and then summarized all Boolean belongings of this point across a wide range of DEM resolutions into fuzzy memberships to these classes. This multi-scale approach is semantically (categorically) explicit, but unable to link typicality of produced landforms to terrain surface shape (e.g. steepness). Lucier and Stein (2005) used an expanding circular ring to characterize the central point by accumulating the sign of elevation difference between the central point and equally spaced points on the ring. Multi-scale summit points could then be identified as having the highest accumulated number of positive signs. This approach also ignores local variability in topographic shape (e.g. between rings and sample points). It produces crisp landform objects, and the ring-based sampling scheme may not be representative enough when the ring is greatly enlarged, especially in a complex landscape.

Hence, there has been a growing trend of considering higher-scale topographic contexts in landform classification, in which an expanding window is often employed (e.g. MacMillan *et al.* 2000, Schmidt and Hewitt 2004; also see Mackay *et al.* 1992). However, a key challenge persists regarding how to characterize local variability in combination with wider contexts, and to describe broad contexts without losing local (or smaller-scale) details. This indicates a need of combining multi-scale considerations with multiple criteria and with the spatial continuity of topography.

3. Methods

3.1 Characteristics of the procedure

The procedure described in this paper employs a similar approach to the MRVBF (multi-resolution valley bottom flatness) index of Gallant and Dowling (2003). MRVBF uses slope that is calculated with DEMs of coarsening resolutions (with a correspondingly decreasing slope threshold) and elevation percentile that is calculated with an expanding window. Slope is inverted into a flatness index, and the elevation percentile is inverted into a lowness index. The two indexes are combined by multiplication at each scale to give the valley bottom flatness (VBF) of that scale. VBF is then summarized across a range of considered (and weighted) scales to produce the value of MRVBF representing the multi-scale membership to valley bottoms. Thresholds of MRVBF may define boundaries of valleys, but the

internal variability of these valleys is retained. In this way, MRVBF translates semantic meanings of valley bottoms first into quantifiable terrain attributes (indexes) at multiple scales, and then into fuzzy landform objects with modifiable boundaries.

The procedure in this paper also presents several differences from MRVBF. First, with the expansion of considered context (scale), it does not generalize the DEM to save computation time because in the rugged landscape, in contrast to relatively flat valley bottoms, summit definitions and terrain attributes may vary dramatically with DEM resolution change (Deng *et al.* 2007). Dealing with a fine-resolution DEM throughout the procedure necessarily affects the computation speed and limits the number of considered scales.

Second, MRVBF is directly calculated from topographic attributes, but the procedure in this paper first derives multi-scale peak class centres and then uses them to calculate peakness, or peak prototypicality and similarity (Fisher *et al.* 2005). In correspondence, the procedure uses an attribute distance function (see equation (4) below), rather than multiplication, to summarize attributes for multi-criteria peakness. This allows flexible incorporation of multiple criteria with modifiable weights and avoids over-sensitivity of peak memberships to one attribute (see equation (2) below).

Third, MRVBF uses a nonlinear function to transform input variables into values ranging between 0 and 1, so that the magnitude of MRVBF may be controlled; but the procedure in this paper uses a statistical transformation in consideration of the study area context (see equations (2) and (5) below). This necessarily implies that: (1) peakness falls between 0 and 1; and (2) peakness is more closely tied to and more dependent on the studied landscape situation than MRVBF that may need adjustments of parameters (e.g. thresholds, scale factors, etc.) for its adaptation to specific landscapes.

3.2 Case-study area and data

A $17.4 \times 9.3 \text{ km}^2$ area in the Santa Monica Mountains, California, was chosen for the case study (figure 1). This area is characterized by steep slopes, high relief (more than 940 m), and rugged, deep-cutting fluvial topography. A visual interpretation of

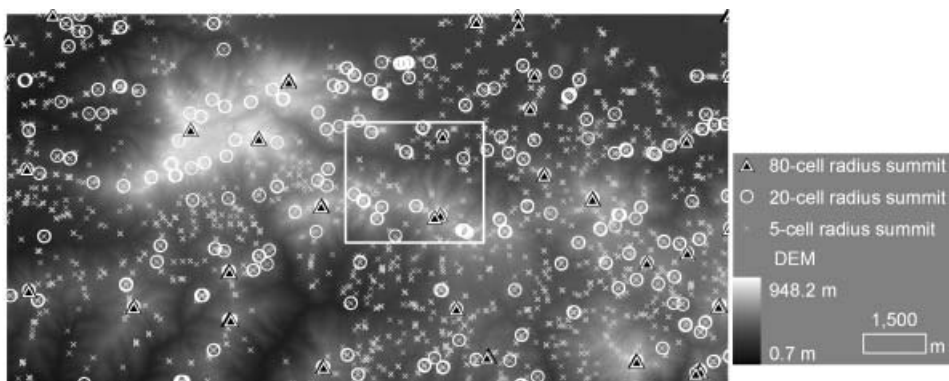


Figure 1. Study area DEM and summit cells identified with moving circular windows of three radii: five cells, 20 cells, and 80 cells. The white inset box indicates the area shown in figures 2, 3, and 6(a).

the study area DEM indicates that mountain peaks in this small study area vary greatly in terms of elevation, relief, shape, size, steepness, isolation/connectedness, etc. A USGS 10 m DEM was used for the case study. All computations were carried out in ArcGIS 9.0 on a desktop computer using existing functions of the software.

3.3 Identify summit points

An expanding circular window—signifying a higher scale or growth of spatial contexts—helps identify candidate summit cells on a DEM using maximum elevation and high relief (above a pre-specified threshold) in the window as the criteria. The threshold relief determines the number of candidate summits, many of which will be found to have low peakness, even though they are selected as summits, thus minimizing the effect of this threshold. Larger relief thresholds are chosen for larger window sizes. Analysing on a continuous range of spatial scales would produce an ideal representation of the scale effect, but large window sizes would tremendously increase the time used for cell-by-cell neighbourhood computations, especially on high-resolution DEMs (e.g. ≤ 10 m). This factor limited the number of windows tested in the case study.

The case study used three circular moving windows—with five-cell, 20-cell, and 80-cell radii—to represent change of spatial scales. Relief thresholds of 20 m were used for five-cell windows, and 80 m for 20-cell and 80-cell windows. In all, 3542 cells were identified to be summits with the five-cell radius windows, 562 with the 20-cell radius, and 121 with the 80-cell radius. Many of the summit cells neighbour each other (indicating flat hilltops on the 10 m DEM), so there appear to be far fewer summit cells on the map (figure 1). Larger windows and the higher relief threshold produced fewer summits, which appear at more prominent topographic locations.

3.4 Characterize peaks

Four semantic meanings of the prototype peak are identified and then imported into the procedure based on the expert knowledge. A typical peak would be the summit that: (1) has high down-slope relief in a local area; (2) is steep in this local area; (3) has high elevation in comparison with a large surrounding neighbourhood (e.g. much larger than the local area in (1) and (2)); and (4) does not have many competing peaks in this large neighbourhood. The first two describe inherent morphometric properties of peaks, whereas the latter two are for topographic contexts. These properties are applicable to non-summit points, too, making peaks comparable with the landscape background. It is nevertheless important to note that, without identifying and importing the ‘peak’ central concept, these four properties are insufficient in depicting peak memberships and boundaries. For example, many steep slopes satisfy the first and second criteria, mountain-top plateaus satisfy the third, and low-lying basins satisfy the fourth criterion. This point is demonstrated in the case study (e.g. figure 2).

The four properties are quantified next. Down-slope relief is calculated as the difference between the central cell elevation and the minimum elevation in a local circular window (the same as that used to identify summit points); steepness is as the mean slope of all cells within this window. High elevation and lack of competing peaks are quantified using a much larger window (three times larger in the case study). The third property, altitude height, is represented with a relative altitude (H_s)

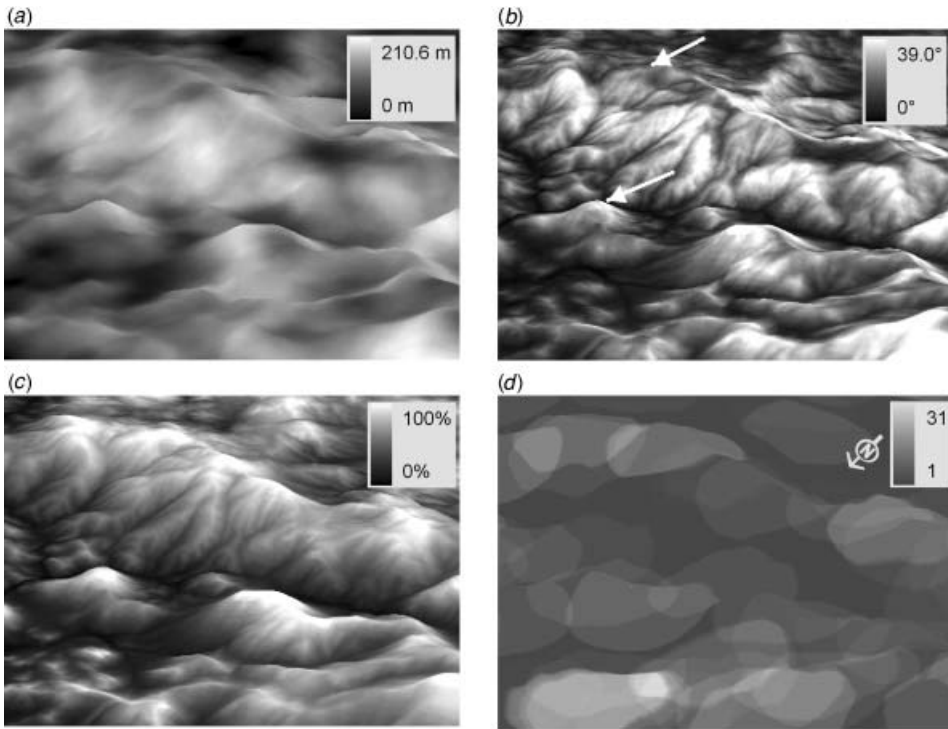


Figure 2. Peak attributes corresponding to summits identified with the 20-cell radius moving window: (a) local relief; (b) local mean slope; (c) relative altitude in a large surrounding neighbourhood; and (d) number of summit points in the surrounding neighbourhood. The area covers the inset box in figure 1 (viewed roughly from a NNW direction), and the properties are draped on the 10-m DEM (with a vertical exaggeration of 1.27 times).

that is calculated from the summit elevation (E_s), the maximum elevation (E_{\max}), and the minimum elevation (E_{\min}) in the large window:

$$H_s = \frac{E_s - E_{\min}}{E_{\max} - E_{\min}} \times 100 \quad (1)$$

H_s calculation is very time-consuming with large windows. For example, it took more than 10 h on a desktop computer to calculate H_s for the summits identified with the 80-cell radius window in the case-study area (of about 1.61×10^6 cells). Generalizing DEM would increase the computation speed but would result in loss of summits and decaying precision of summit locations and relief in this procedure, so that the computation of neighbouring summits and H_s would both be problematic. In addition, the topographic meanings of local peak properties would be changed in the process of generalizing DEMs (e.g. see Deng *et al.* 2007) since one large cell on the generalized DEM may contain (or hide) important 'local' variability in the peak area. The fourth property is represented with the count of summits in the large window because the prominence of a peak identified in a $10\,000\text{ m}^2$ area may be influenced by other nearby (e.g. $<300\text{ m}$) peaks, but not by peaks located too far away.

Figure 2 presents the above four peak properties for the case-study area corresponding to 20-cell radius summits. The primary role of these properties is to distinguish more prominent peaks from others. For example, the relative flatness of mountain-top summits (e.g. the upper arrow in figure 2(b)) may prohibit the summits from gaining a higher peakness at this scale than a lower but steeper summit (e.g. the lower arrow in figure 2(b)). The prominence of this lower summit, however, may in turn be affected by its moderate altitude characterized at a coarser scale.

3.5 Calculate peak prototypicality

The four peak properties are summarized into the peak prototypicality (φ_j), ranging between 0 and 1, at each (j th) scale:

$$\varphi_j = \sum_{i=1}^n \frac{w_i (a_{ij} - \min a_{ij})}{(\max a_{ij} - \min a_{ij})} \quad (2)$$

where $\max a_{ij}$ and $\min a_{ij}$ are the maximum and minimum of property a_i among all summit points identified at the j th scale, a_{ij} is a_i for each summit at the j th spatial scale, n is the number of properties, and w_i is the weight of the i th attribute ($\sum w_i = 1$). The inverse value of the number of neighbouring summits (plus one, as some points have no neighbouring peaks) is used in this calculation. When a particular peak property needs to be emphasized, it may take a higher weight. Allowing weights of these properties to be modifiable would help integrating particular human purposes and situations, so as to partly address the ‘higher-order’ vagueness issue (Fisher *et al.*, in press; also see Deng *et al.*, 2006, for the effects of attribute weights), but this possibility is not tested in the case study.

The case study adopted a uniform weight for the four peak properties. The resultant φ_j effectively differentiated the prototypicality of summits at three spatial scales (figure 3). A prominent summit at a fine scale may not be prominent at a

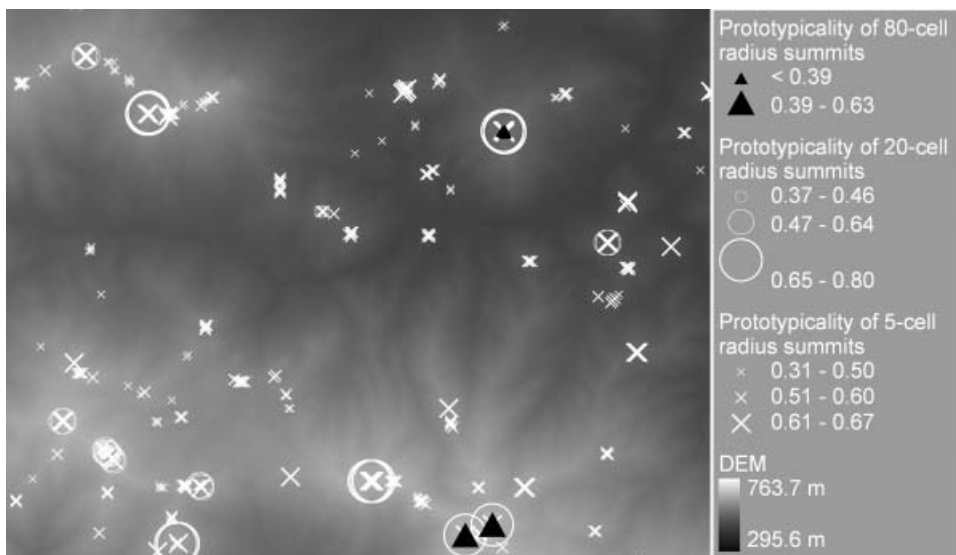


Figure 3. Individual-scale peak prototypicality for five-cell, 20-cell, and 80-cell radius summits of the inset area in figure 1, with a 10-m DEM background.

coarser scale, and vice versa. High prototypicality summits may not be exclusively contained in high-elevation areas.

3.6 Summarize peak prototypicality across scales

Peaks may appear differently when observation scale varies (e.g. figure 3), and the overall typicality of a summit can be evaluated by summarizing φ_j across all considered spatial scales into a single value φ . Two rules are established in so doing: (1) summits identified at all scales are recognized (with a non-negligible weight) in the summarizing process; and (2) coarser scales produce more important summits, thus receiving higher weights. φ is written as:

$$\varphi = \frac{\sum_{j=1}^m (w_j \times \varphi_j)}{\sum_{j=1}^m w_j} \quad (3)$$

where w_j is the weight of scale j , and m is the total number of scales considered.

Large differences between weights of scales would cause φ to rely heavily on peaks identified at coarse scales, resulting in a loss of local variability in peakness. The effect of varying scales weights will be discussed in section 3.7.4. Weights of 1, 1.2, and 1.4 were selected in the case study for summits with five-cell, 20-cell, and 80-cell radius windows. Based on φ of summit points, many (but not all) prominent peaks were identified along the central ridgeline (figure 4). The consideration of topographic context (H_s and number of neighbouring peaks) allowed the distinction between more important peaks and numerous others along this central ridgeline. A maximum prototypicality measure of only 0.70 was obtained because the adopted peak properties did not co-vary from peak to peak, and/or from scale to scale.

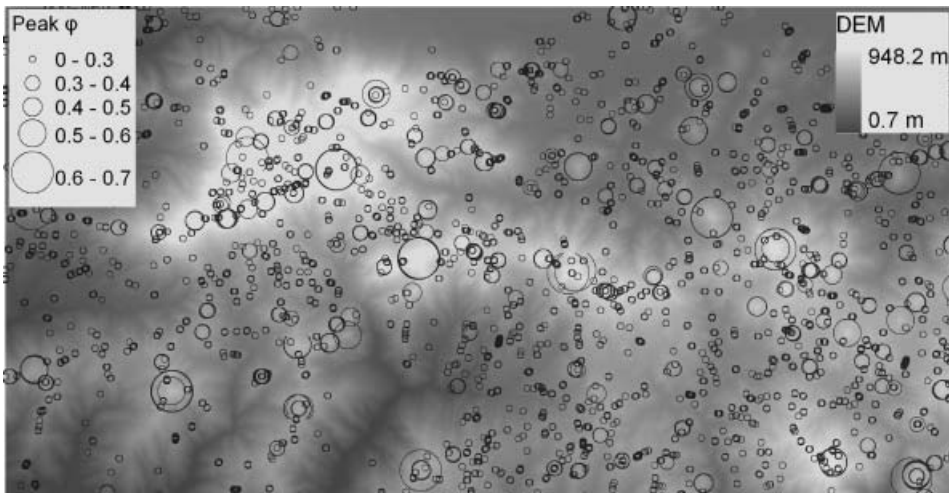


Figure 4. Overall peak prototypicality across three considered spatial scales for all summit cells identified at these scales.

3.7 Evaluate similarity to peaks

The previous steps identify peaks as summit *points* and evaluate their prototypicality, and the following steps will expand the idea and map peaks as fuzzy areal objects with modifiable boundaries.

3.7.1 Peak class centre. A threshold φ_j is specified to select the most typical summits or peak prototypes at each spatial scale. The peak class centre is then calculated as the mean properties of prototype peaks. The case study used the top 20% φ_j to identify prototype peaks and to calculate the peak class centre (table 1), which tends to have a high relief, steep slope, high relative altitude, and small number of competing peaks (e.g. in reference to figure 2). With the coarsening of spatial scales, peak class centres show an obvious increase in relief and decrease in slope and relative altitude, all due to the rugged mountainous terrain of the study area. Other thresholds of φ_j were tested, too, and a decreasing threshold increased local relief, slope, and non-local relative altitude of class centres, but did not cause a trended change for the number of neighbouring peaks. The effect of this threshold on peakness will be explained in section 3.7.4.

3.7.2 Similarity to peak class centre. The four peak properties are used to calculate the similarity of each point to a scale-specific peak class centre in two steps: first, calculating an attribute distance between each point and a peak class centre, and second, converting the attribute distance into a relative similarity measure. The case study used the diagonal norm distance function. At the j th spatial scale, the attribute distance (d_{kj}) between a grid point k and the j th class centre is calculated as:

$$d_{kj} = \sqrt{\sum_{i=1}^n \frac{1}{\sigma_{ij}^2} (a_{ik} - \bar{a}_{ij})^2} \quad (4)$$

where σ_{ij} is the standard deviation of property a_i at the j th spatial scale, a_{ik} is the value of the property a_i for point k at the j th spatial scale, \bar{a}_{ij} is the j th peak class centre value for property a_i , and n is the number of properties used. A larger d_{kj} signifies less similarity between a point and a peak class centre, and, for the easiness of interpretation, d_{kj} is converted into a membership μ_{kj} whose value ranges from 0 (different) to 1 (the same):

$$\mu_{kj} = \frac{\max d_j - d_{kj}}{\max d_j - \min d_j} \quad (5)$$

where $\max d_j$ and $\min d_j$ are the maximum and minimum attribute distances between the j th class centre and all grid points across the entire area.

Table 1. Attributes of peak class centres for summit cells identified at three spatial scales.

	Radius of local moving window (cell)					
	5	15	20	60	80	240
Window size for peak identification						
Window size for attribute calculation	5	15	20	60	80	240
Local relief (m)	55.9		145.6		392	
Local mean slope (°)	35.7		30.2		24.7	
Relative altitude (%)		97.8		96.4		91.9
Number of neighbouring peaks		3		7		6

Figure 5 shows the μ_{kj} of the case-study area at three spatial scales. Focus on the local variability at a fine spatial scale (figure 5(a)) produced a more heterogeneous variability of peakness, which differentiated local contexts and shape of peaks but did not distinguish between ‘peaks for hills’ and ‘peak for the mountain’. This second goal was reached by the coarse-scale peakness (figure 5(c)), on which contiguous, prominent high-peakness areas were formed in the high-elevation ridgeline area. The production of these peakness patterns makes it possible to combine various spatial scales that characterize both local variability and high-order contexts.

3.7.3 Peak class membership across scales. In a similar way to equation (3), μ_{kj} is summarized across all considered spatial scales to produce an overall peak membership μ_k for each point k :

$$\mu_k = \frac{\sum_{j=1}^m (w'_j \times \mu_{kj})}{\sum_{j=1}^m w'_j} \quad (6)$$

where w'_j is the weight of the j th scale, and m is the number of scales considered. Heavier weights should again be given to coarser spatial scales.

Calculation of μ_k for the case-study area used the same set of weights for w'_j as for w_j in equation (3), and the results strongly pronounced the difference between peak and non-peak areas, especially along the central ridgeline (figure 6). However, each point—even the valley bottom—has a non-zero similarity to peaks, allowing peakness comparison across the entire landscape. Some high-elevation points presented low μ_k values (figure 6(a)) because they have poorer peakness properties (e.g. shape, position, and context).

3.7.4 Effect of varying w'_j and threshold φ_j on μ_k . Three groups of cells across an adjacent hill-valley transect were visually selected on a 10 m DEM to test the effects of varying threshold φ_j and w'_j on μ_k . They include five neighbouring summit cells (525–527.5 m in elevation), seven neighbouring hillslope cells (431.1–435.8 m), and 25 neighbouring valley bottom cells (303.3–303.9 m). Six thresholds of φ_j were tested for their effect on varying class centres (section 3.7.1) and hence μ_k —2%, 5%, 10%, 15%, 20%, and 30%—and the results are presented in figure 7(a). Increasing threshold φ_j has apparently decreased the μ_k contrast between peaks and valleys, and caused more sensitive response (consistently increasing μ_k) on valley/slope cells than on summit cells. Summit cells did not respond until threshold $\varphi_j > 10\%$ and had only a slight decrease in μ_k . Five w'_j combinations were tested for equation (6). For five-cell, 20-cell, and 80-cell radii (in that order), they are respectively: (1) 1, 1, 1; (2) 1, 1.2, 1.4; (3) 1, 1.5, 2; (4) 1, 2, 3; and (5) 1, 3, 5. With the increase of coarse scale weights, the μ_k contrast between summit cells and valley/slope cells decreased; valley cells seemed to be the most sensitive and presented consistent μ_k increase; μ_k change of summit cells is minor with a weak decreasing trend (figure 7(b)).

3.8 Delineating boundaries for peak entities

Acting in the same way as an α -cut in the fuzzy set theory (Cheng 2002, Robinson 2003), thresholds of μ_k can be easily translated into modifiable belongingness of k to a peak and helps delineating peak entities as high μ_k areas with fuzzy (or adjustable)

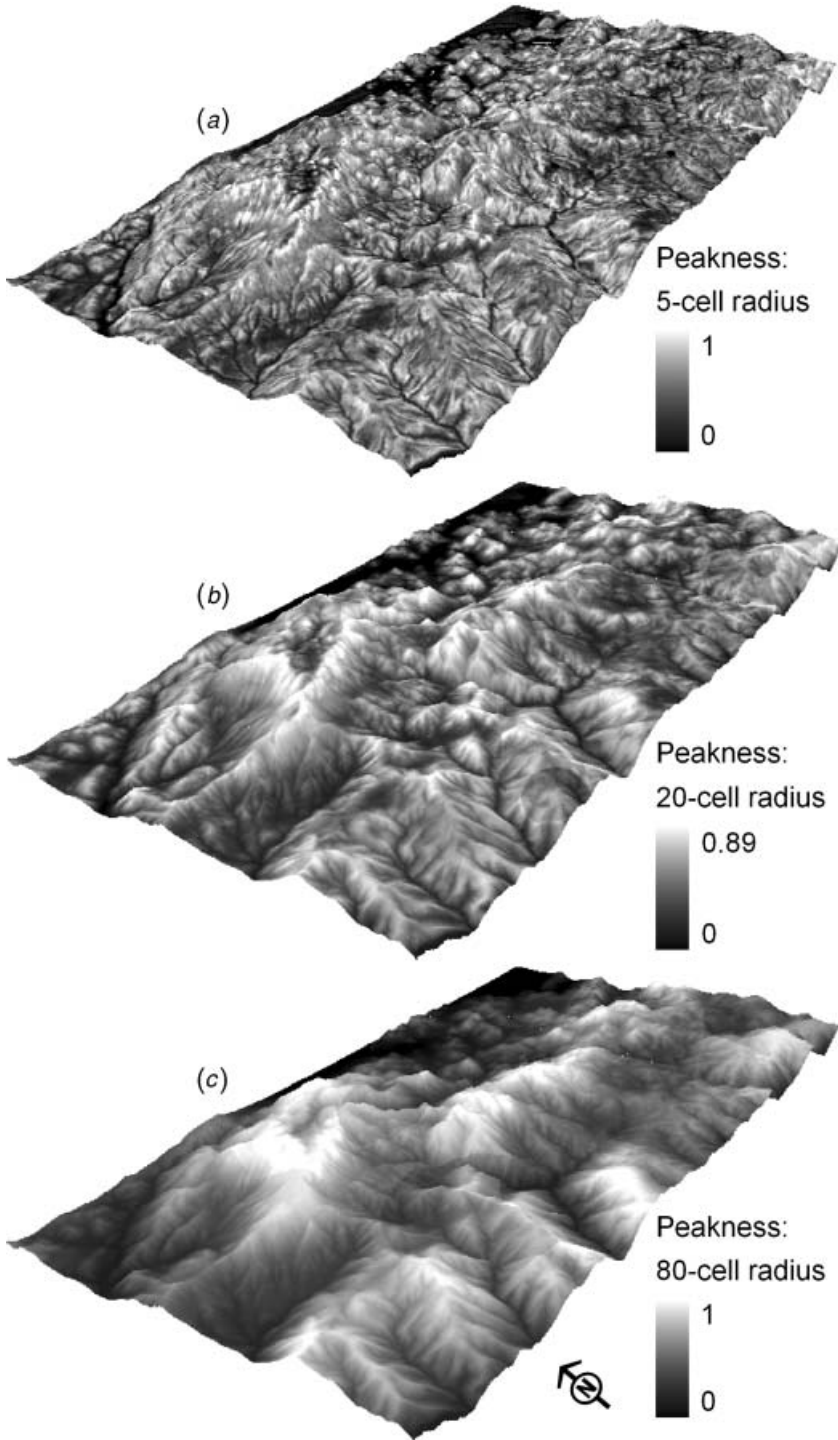


Figure 5. Distribution of similarity to peak class centres (peakness, or μ_{kj}) defined at three spatial scales, corresponding to five-cell radius window summits (a), 20-cell radius window summits (b), and 80-cell radius window summits (c). The raster layers are draped on the 10-m DEM with a vertical exaggeration of 1.61 times.

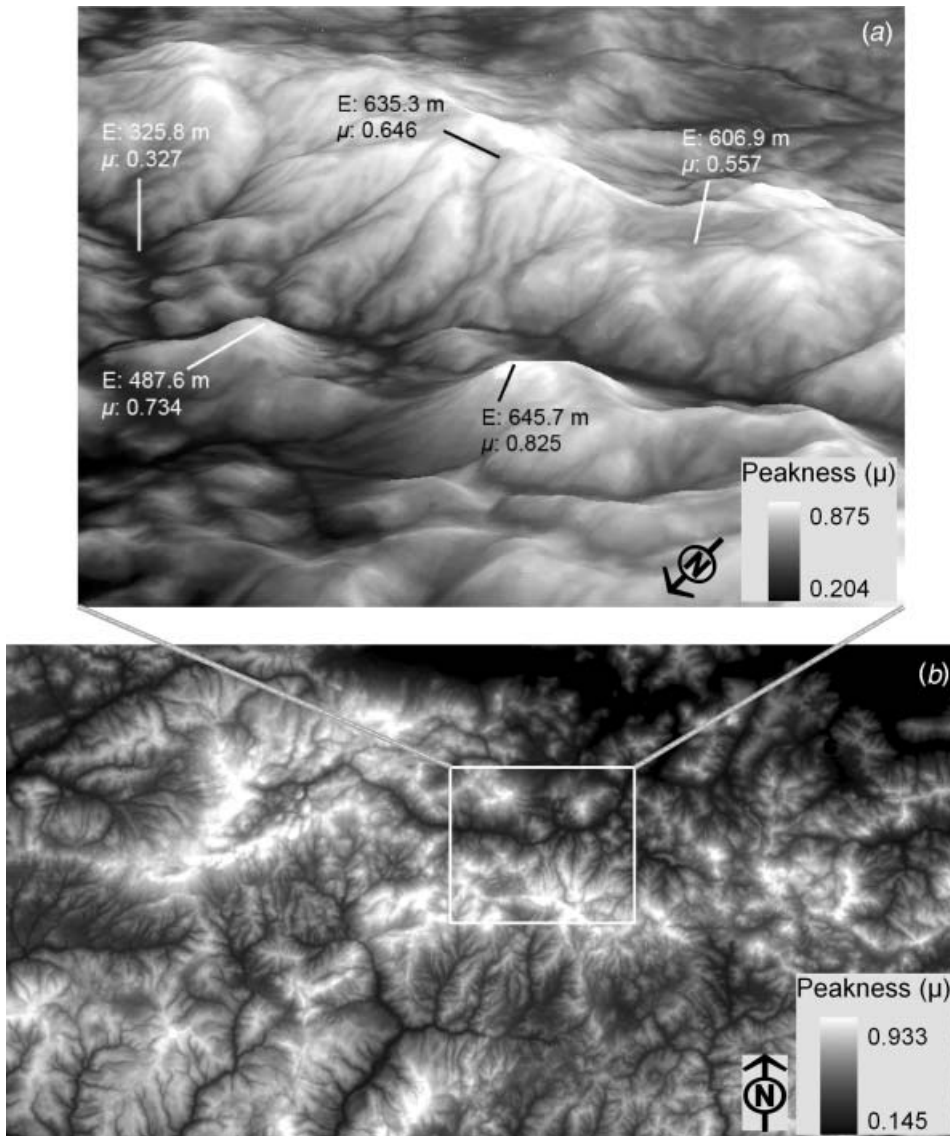


Figure 6. Distribution of overall peakness (μ_k) summarized across the three considered spatial scales: (a) the inset area in figure 1 draped on 10-m DEM (with a vertical exaggeration of 1.27 times and a roughly NNW viewing direction; E is elevation); and (b) the entire area.

boundaries. A threshold of μ_k corresponds to both peak entity size and peak entity properties, making it an exploratory tool for peak delineation (e.g. figure 8). Peak entities may be viewed as uniform objects characterizing statistical summaries (e.g. mean) of μ_k , μ_{kj} , and peak properties (section 3.4). The internal variability of peak entities may in the mean time be retained as separate raster layers. Four μ_k thresholds—0.80, 0.74, 0.70, and 0.65—defined four sets of enlarging peak entities in the case-study area (figure 8). With a very high threshold μ_k , only the most typical peaks were depicted covering a small area that concentrated along the central

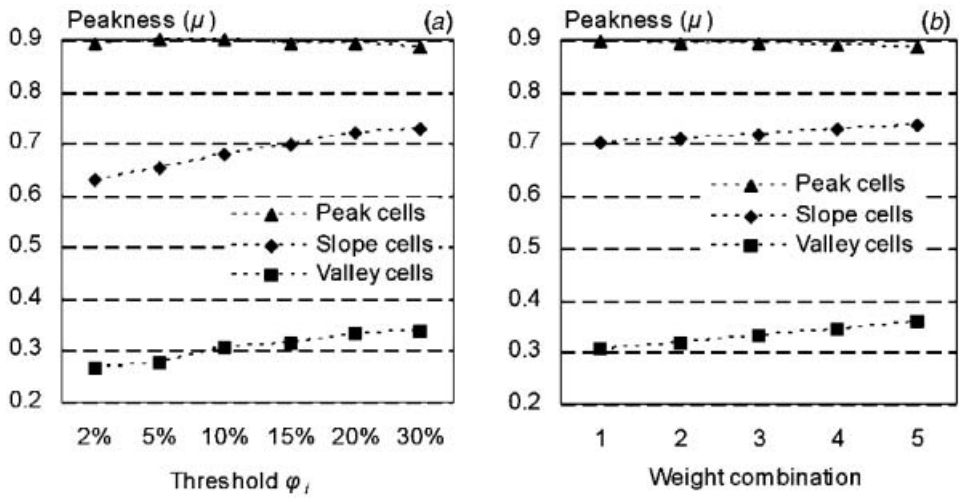


Figure 7. Sensitivity of peakness (μ_k) to threshold peak prototypicality ϕ_j (a) and weights of scale w_j' (b), assigned using five weight combinations (see section 3.7.4). The sensitivity is demonstrated with three sets of cells representing peaks, hillslopes, and valleys.

ridgeline. A lowering threshold μ_k would allow peaks to grow into fuzzy peak regions. Three meanings of fuzziness were thereby implemented: (1) adjustability of peak boundary; (2) variable typicality of a peak region in terms of average or minimum μ_k ; and (3) non-uniform contents of peak regions.

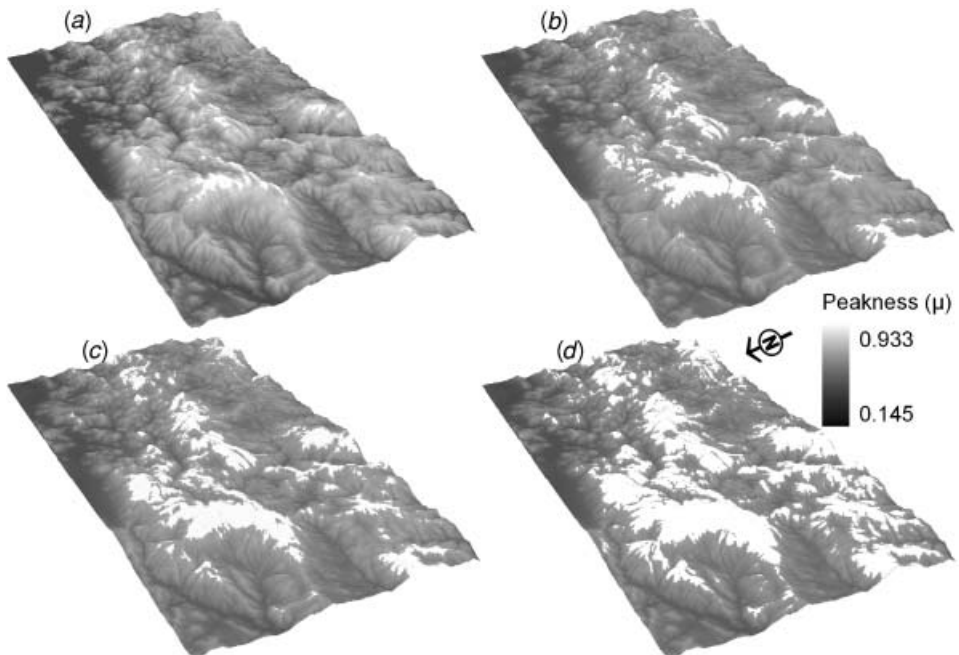


Figure 8. Peak regions (white areas), or peak entities, delineated based on four threshold memberships of overall peakness: 0.80 (a), 0.74 (b), 0.70 (c), and 0.65 (d). The background greyness represents peakness (μ_k), which is draped on the 10-m DEM with a vertical exaggeration of 1.61 times.

4. Discussion

- The consideration of multiple spatial scales has been combined with weighted summary of spatial scales, and attention is paid to the topographic context (e.g. number of neighbouring peaks), position (e.g. relative altitude), as well as the shape (e.g. slope and local relief) of the peaks. All these helped the depiction of contiguous yet internally variable peak entities.
- The derivation of summits, peak properties, φ_j , μ_{kj} , and class centres is all based on the consideration of the entire study area, and μ_k is consequently specific for the landscape where it is derived.
- As mentioned in section 3.2, the slow computing speed incurred by large neighbourhood windows is a weakness of the procedure, especially for peak delineations of large areas. Since generalizing DEMs may incur undesirable effects in this procedure, a more satisfactory solution for this problem has yet to be found.
- Large moving windows used for peak property calculation will be incomplete along DEM edges, causing distortions to the output. A wide DEM margin should be included for the calculation of peak properties, but excluded from further analysis. For example, the use of a 240-cell radius circular window on a 10 m DEM—necessary for the characterization of 80-cell radius peaks—means that only the area farther than 2.4 km from the edge would not be influenced by the edge effect, and more severe distortions would appear near the edge, as exemplified by the two questionable, high-prototypicality summits along the eastern edge in figure 4.

5. Conclusions

A procedure was proposed that combines multiple spatial scales and multiple semantic meanings to delineate mountain peaks as fuzzy entities, which have flexible boundaries, fuzzy typicality, spatially contiguity, and non-homogeneous contents. Memberships to a multi-scale, multivariate peak class centre were derived to represent the spatial continuity of the terrain surface, or gradation of feature boundaries. The scale dependency of peaks was addressed by a consideration of both individual scales and scale-to-scale connections. Not only the local peak properties but also the topographic position and contexts of the peaks were considered. Weights of peak properties and spatial scales, and thresholds of peakness for peak boundaries were all modifiable, making it possible to develop purpose-oriented mapping of mountain peaks. Hence, the procedure has the potential of bridging qualitative peak meanings to quantitative definitions and geographic delineations of peaks.

Acknowledgements

Mr Bård Romstad, University of Oslo, and Mr Rahul Chabuskar, University of Southern California, participated in the early process of idea development. Professor Peter Fisher, City University of London, provided valuable comments. Suggestions from three reviewers and Professor Mark Gahegan, Pennsylvania State University, greatly improved the manuscript quality.

References

- BURROUGH, P.A. and McDONNELL, R.A., 1998, *Principles of Geographical Information Systems*, pp. 265–291 (Oxford: Oxford University Press).
- CHENG, T., 2002, Fuzzy objects: Their changes and uncertainties. *Photogrammetric Engineering and Remote Sensing*, **68**, pp. 41–49.
- DENG, Y., WILSON, J.P. and BAUER, B.O., 2007, DEM resolution dependencies of terrain attributes across a landscape. *International Journal of Geographical Information Science*, **21**, pp. 187–213.
- DENG, Y., WILSON, J.P. and SHENG, J., 2006, Effects of variable attribute weights on landform classification. *Earth Surface Processes and Landforms*, **31**, pp. 1452–1462.
- FISHER, P.F., CHENG, T. and WOOD, J., 2007, Higher order vagueness in geographical information: Empirical geographical population of type n fuzzy sets. *Geoinformatica* (DOI: 10.1007/s10707-006-0009-5).
- FISHER, P.F., WOOD, J. and CHENG, T., 2004, Where is Helvellyn? Fuzziness of multi-scale landscape morphometry. *Transactions of the Institute of British Geographers*, **29**, pp. 106–128.
- FISHER, P.F., WOOD, J. and CHENG, T., 2005, Fuzziness and ambiguity in multi-scale analysis of landscape morphometry. In *Fuzzy Modelling with Spatial Information for Geographic Problems*, F.E. Petry, V.B. Robinson and M.A. Cobb (Eds), pp. 209–232 (New York: Springer).
- GALLANT, J.C. and DOWLING, T.I., 2003, A multiresolution index of valley bottom flatness for mapping depositional areas. *Water Resources Research*, **39**, pp. 1347–1359.
- GRAFF, L.H. and USERY, E.L., 1993, Automated classification of generic terrain features in digital elevation models. *Photogrammetric Engineering and Remote Sensing*, **59**, pp. 1409–1417.
- LUCIEER, A. and STEIN, A., 2005, Texture-based landform segmentation of LiDAR imagery. *International Journal of Applied Earth Observation and Geoinformation (JAG)*, **6**, pp. 261–270.
- MACKAY, D.S., ROBINSON, V.B. and BAND, L.E., 1992, Classification of higher order topographic objects on digital terrain models. *Computers, Environment, and Urban Systems*, **16**, pp. 473–496.
- MACMILLAN, R.A., PETTAPIECE, W.W., NOLAN, S.C. and GODDARD, T.W., 2000, A generic procedure for automatically segmenting landforms into landform elements using DEMs, heuristic rules and fuzzy logic. *Fuzzy Sets and Systems*, **113**, pp. 81–109.
- MARK, D.M. and SMITH, B., 2004, A science of topography: Bridging the qualitative–quantitative divide. In *Geographic Information Science and Mountain Geomorphology*, M.P. Bishop and J. Shroder (Eds), pp. 75–100 (Chichester, UK: Springer-Praxis).
- ROBINSON, V.B., 2003, A perspective on the fundamentals of fuzzy sets and their use in Geographic Information Systems. *Transactions in GIS*, **7**, pp. 3–30.
- SCHMIDT, J. and HEWITT, A., 2004, Fuzzy land element classification from DTMs based on geometry and terrain position. *Geoderma*, **121**, pp. 243–256.
- SMITH, B. and MARK, D.M., 2003, Do mountains exist? Ontology of landforms and topography. *Environment & Planning B: Planning and Design*, **30**, pp. 411–427.
- USERY, E.L., 1996, A conceptual framework and fuzzy set implementation for geographic features. In *Geographic Objects with Indeterminate Boundaries*, P.A. Burrough and A.U. Frank (Eds), pp. 71–86 (London: Taylor & Francis).
- WOOD, J., 1998, Modelling the continuity of surface form using digital elevation models. In *Proceedings of the 8th International Symposium on Spatial Data Handling*, T. Poiker and M. Chrisman (Eds). Simon Fraser University, Burnaby, British Columbia, pp. 725–736.
- WOOD, J., 2004, A new method for the identification of peaks and summits in surface models. In *Proceedings of GIScience 2004—The Third International Conference on Geographic Information Science*, Adelphi, MD, pp. 227–230.